IN SITU OBSERVATION OF TRICALCIUM ALUMINATE DISSOLUTION IN WATER

Shaoxiong Ye (1), Pan Feng (1,2), Yao Liu (1) and Jiaping Liu (1,2)

(1) Jiangsu Key Laboratory of Construction Materials, School of Materials Science and Engineering, Southeast University, Nanjing 211189, China

(2) State Key laboratory of High Performance Civil Engineering Materials, Nanjing 210008, China

Abstract

The nanoscale dissolution flux of tricalcium aluminate (C_3A) in flowing water is characterized in situ by Digital Holographic Microscopy (DHM). The pure dissolution of C_3A in flowing water with a flow rate of 34 $ml \cdot min^{-1}$ before the precipitation of hydrated phases only lasted about one quarter of a second, and the pure dissolution rate mostly falls in the range of 500 ~ 1500 $\mu mol \cdot m^{-2} \cdot s^{-1}$. Subsequently, foil shape hydration product formed and rapidly covered the surface of C_3A, leading to the dramatic decrease of the overall dissolution rate to 55 ± 10 $\mu mol \cdot m^{-2} \cdot s^{-1}$.

Keywords: C_3A, rapid dissolution, DHM

1. INTRODUCTION

Mineral dissolution is a key process in geochemical reactions and environmentally relevant processes[1]. In recent years, the dissolution behaviors of cement clinkers have been obtaining increasing attention[2-5]. Portland cement is a low-cost material with multi minerals, including alite, belite, tricalcium aluminate (C_3A), gypsum, etc. The hydration of cement, which is a complex reaction that combines with mineral dissolution and product precipitation, is the origin of strength and determines other properties of cement paste. According to Julliand et al[2], dissolution plays an important role in alite hydration, and the change of alite dissolution mechanism is responsible for the onset of induction period. Similarly, Nicoleau & Nonat[5] proposed that dissolution of C_3S is the rate controlling step in the early hydration based on the change of saturation index of C_3S.

Besides alite, C_3A is also a key component of Portland cement. Though its content is much lower than alite, it has an important effect on early properties of cement paste, especially for the workability[6]. Because C_3A has a much higher reactivity than alite, it reacts much faster with water than C_3S, which makes it an even bigger challenge to measure its dissolution rate in water. To slow down the dissolution rate of C_3A, Brand and Bullard[7] lowered the water activity by incorporating ethanol in water and measured the dissolution rate in solutions with

high content of ethanol. However, the presence of ethanol is likely to change the dissolution mechanism of C_3A due to its adsorption to the C_3A surface[8-9]. Thus, how the dissolution rate of C_3A in the mixture solutions is related to that in water still remains unresolved.

The Digital Holographic Microscopy (DHM) is a new technique that is able to detect the evolution of surface elevation, which can provide insights about dissolution mechanisms that would be valuable in cement research, like determining the reactivities of clinker and supplementary cementitious materials, exploring the effect of admixtures on cementitious materials, etc. For the purpose of measuring net dissolution rate of C_3A in water, which is helpful in understanding the early age hydration of cement, this paper uses DHM to monitor the surface height change of polished C_3A samples on nano-scale. Because of the unique capability of fast image collection of DHM, the real-time observation of fast dissolution is realized.

2. MATERIALS AND METHODS

2.1 C_3A pellets sintering

C_3A pellets were produced in lab through hot-press sintering method by spark plasma sintering (HP-D5, FCT). A schematic plot of sintering procedure is shown in Figure 1. The detailed information for C_3A pellets sintering is as follows:

Firstly, about 3 g of C_3A powder (purchased from Zibo Ceramic Institute, China) was placed into a graphite die (20 mm in diameter) and pre-pressed by top and down punches. Graphite foil was used to wrap the powder for easy demolding.

Secondly, SPS sintering was carried out to densify the pellet samples. The sintering parameters adopted in this paper was obtained by trial and error. In details, the die was covered by a graphite sleeve and then moved into a vacuum chamber (less than 10 Pa), in which the die was pre-pressed again with a stress of 15 MPa. Then the sample was heated to 1250 °C with a heating rate of 100 °C·min^{-1} and stayed at the maximum temperature for 15 min. Before the temperature reached to 450 °C, the pressure of 15 MPa was applied to the sample, after which the pressure applied was increased at a constant rate from 15 MPa to 40 MPa until the temperature increased up to 1250 °C, and then stayed constantly at 40 MPa at the maximum temperature.

When the heating was done, the sample was rapidly cooled by water cooling system, followed by demolding. The crystal structure of pellet (crushed into powder) was characterized by X-ray diffractometer (Bruker D8, Bruker). The result was shown in Figure 2, indicating the major phase of pellet synthesized was C_3A.

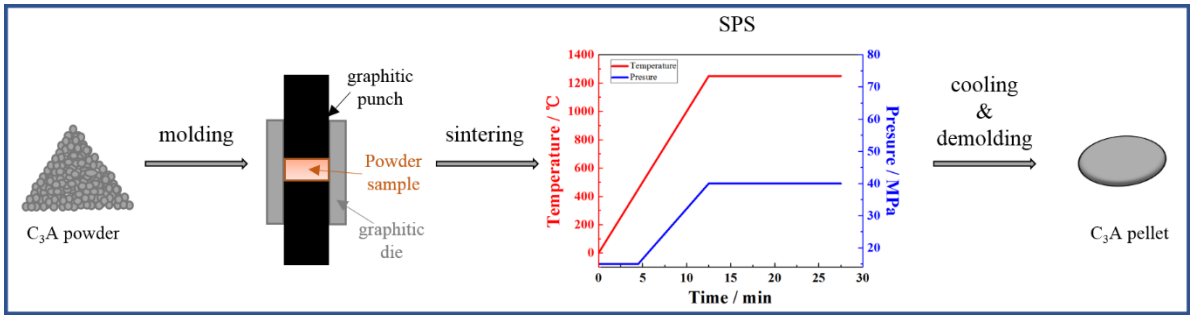

Figure 1: Schematic plot of sintering procedure for C_3A

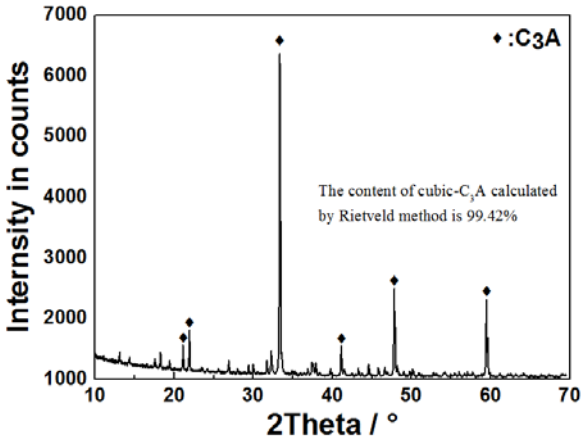

Figure 2: Diffraction pattern of C_3A sample

2.2 DISSOLUTION EXPERIMENTS

C_3A pellets were polished and partially coated with a chemical-inert platinum layer with the thickness of about 20 nm, servicing as a reference plane which is supposed to be unreacted through the whole dissolution measurement. The coating was implemented by applying Turbo-Pumped Sputter Coater (Q150T, JC Nabity). Figure 3 shows one C_3A sample with the coating platinum.

Deionized water was used in all dissolution experiments, and all the experiments were performed following the same method mentioned in [10] at the temperature of 24 ± 1 °C. The DHM (Model R-2203, Lyncée Tec) utilized in this study was operated in the reflection mode. It collected the hologram images of the sample surface at a frequency up to 12.5 s^{-1}. More information about DHM configuration can be found elsewhere[12]. C_3A dissolution was monitored using a 20x immersion objective lens, and the dissolution rate of C_3A, v_{diss}, was determined by dividing the velocity of reactive surface height change by the molar volume of C_3A V_m = 8.91 x 10^{-5} $m^3 \cdot mol^{-1}$

$$v_{diss} = \frac{\Delta h}{\Delta t}\frac{1}{V_m} \quad (1)$$

To reach a condition under which the dissolution is controlled by surface reaction rather than diffusion, the solution was intentionally maintained as diluted as possible by increasing the flow rate of water from 15 up to 55 $ml \cdot min^{-1}$. In this way, conditions far from equilibrium were

obtained. C_3A pellets were produced in lab through hot-press sintering method by spark plasma sintering (HP-D5, FCT). A schematic plot of sintering procedure is shown in Figure 1. The detailed information for C_3A pellets sintering is as follows:

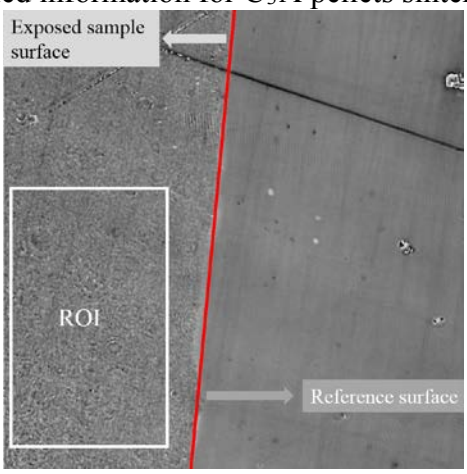

Figure 3: Morphology of partial polished C_3A pellet in phase image obtained by DHM. Reference surface is the surface covered by platinum player. The size of ROI (region of interest) is 220 pixel x 370 pixel, and the size of each pixel is 299 nm x 299 nm

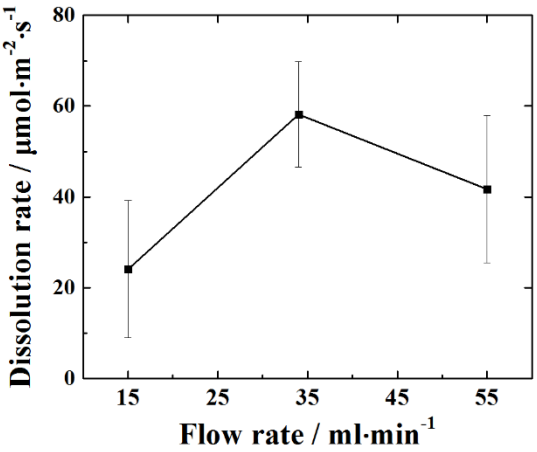

Figure 4: Overall dissolution rate as a function of water flow rate. Error bars are one standard deviation of the average overall dissolution rate for at least three samples at each flow rate

2.3 SURFACE ANALYSIS

Microstructural and morphological characterization of the dissolved surface was carried out using scanning electron microscopy (FEI 3D, FEI). Given that calcium aluminate hydrates form so quickly, C_3A was first dissolved in flowing deionized water with a flow rate of 34 ml·min^{-1} for only about 2 s, and then the surface was washed by ethanol and dried by compacted air as soon as possible. C_3A surface was partially covered with a platinum layer of about 50 nm thickness before immersion as a reference.

3. RESULTS

3.1 FLOW RATE EFFECTS

Figure 4 shows the dependence on flow rate of the overall dissolution rate in the first few seconds. It can be seen that with the increase of flow rate, the measured dissolution rates firstly reach a maximum value at flow rate of 34 ml·min^{-1}, and then drops a little when flow rate continuously increasing. It indicates that when the flow rate is lower than 34 ml·min^{-1}, ionic diffusion may play a more important role than surface reaction in controlling dissolution, and when flow rate is higher, swirls of the water within the flow-through cell might form, resulting the actual flow rate lower than the target value. Therefore, 34 ml·min^{-1} is adopted as the flow rate for the following study.

3.2 SURFACE MORPHOLOGY AFTER INITIAL DISSOLUTION

Surface morphology of C_3A after the contact with water for about 2 s can be seen in Figure 5, in which the right bottom of Figure 5 is the reference surface, and it remains smooth during the measurement, though a few hydration products appears in some local areas. This is due to the incomplete coverage of the platinum player, especially at the regions with deep scratches. Different from reference surface, the surface not covered with chemical-inert layer becomes very rough and a layer of hydration product with crumpled foil shape can be clearly seen, as shown in Figure 6. Similar microstructure changes have been reported by Meredith et al[13]. The thickness of this hydrates layer is measured from the side view of the specimen based on the brightness contrast with the bulk material, as shown in Figure 7. The thickness is about 300 nm.

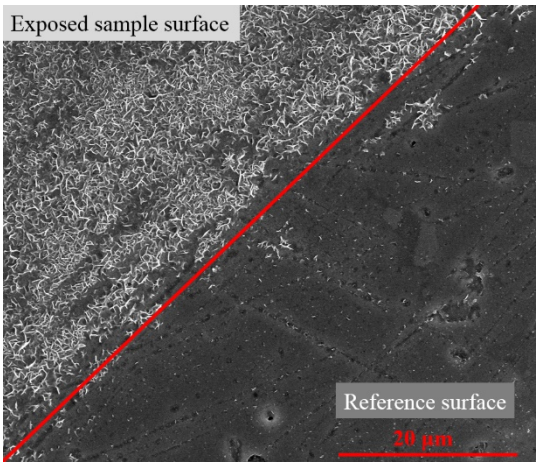

Figure 5: C_3A surface after dissolution

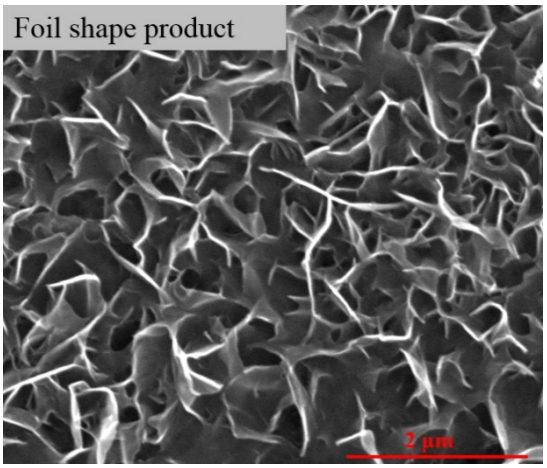

Figure 6: Morphology of hydration product layer

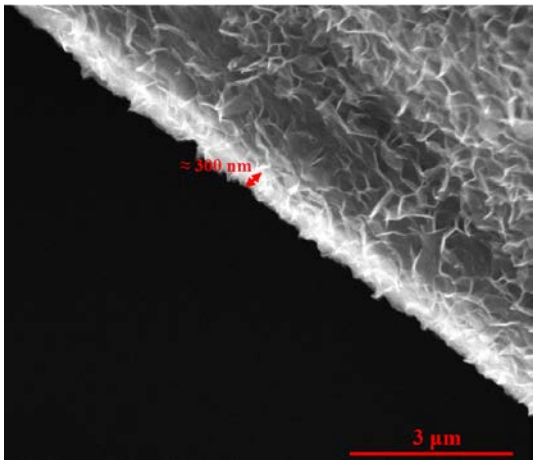

Figure 7: The side view of C_3A surface after dissolution

4. DISCUSSION

4.1 Analysis of C_3A dissolution kinetics

By tracing the average relative surface height change to the reference surface, it is clearly seen in Figure 8 that the surface height changing can be roughly divided into three periods, including the initial fast height reducing, followed by the slow height increasing and the moderate height reducing. It suggests that after the rapid dissolution lasting for about half of a second in the first stage, the surface starts to be gradually covered by the hydration product in the second stage, in agreement with the results shown in Figure 5-7. Though covered by a layer of product, the dissolution continues because the product is with foil shape and not able to stop dissolution completely. Nevertheless, combined by the decreasing effect of dissolution and increasing effect of hydration on surface height change, the average relative surface height decreases at a relative constant rate which is much slower than the initial dissolution. The overall dissolution behavior is similar as the heat flow during C_3A powder hydrates in water[12]. For C_3S and cement, it also can be found in literatures that the heat flow behaves similarly[14-15]. Although it is not completely the same with protective layer hypothesis which assumes a layer formed on the surface can control the hydration reaction for a much longer term, often dozens or hundreds of minutes[16-17], according the DHM measurements, this surface layer was able to decrease the dissolution rate dramatically within the time frame of a quarter of a second.

Figure 9 shows the dissolution rate spectra of region ROI in Figure 3. The rate spectra characterize a frequency distribution of dissolution rates at different locations. They provide much detailed information about the dissolution behavior of a mineral surface and have been widely used in previous studies[10,18]. The positive dissolution rate in Figure 9 means dissolution and the negative means precipitation. Figure 9a shows the overall dissolution rate distribution ranging from -50 to 150 $\mu mol \cdot m^{-2} \cdot s^{-1}$. The precipitation phenomenon is also reported by literature [7], in which the effect of water activity on C_3A dissolution is studied. Different from the overall spectrum, the rates in the first quarter of a second are all positive. More interestingly, the dissolution rates are mostly in the magnitude of 500 ~ 1500 $\mu mol \cdot m^{-2} \cdot s^{-1}$, which are much larger than rates shown in the overall spectrum and the rate extrapolated in literature [7].

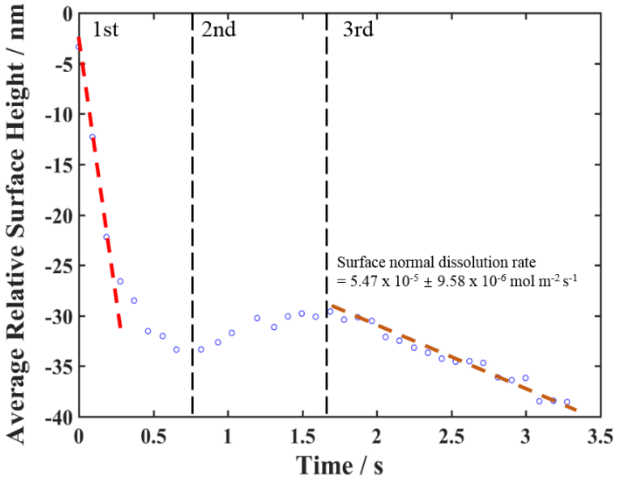

Figure 8: The average surface height change during dissolution

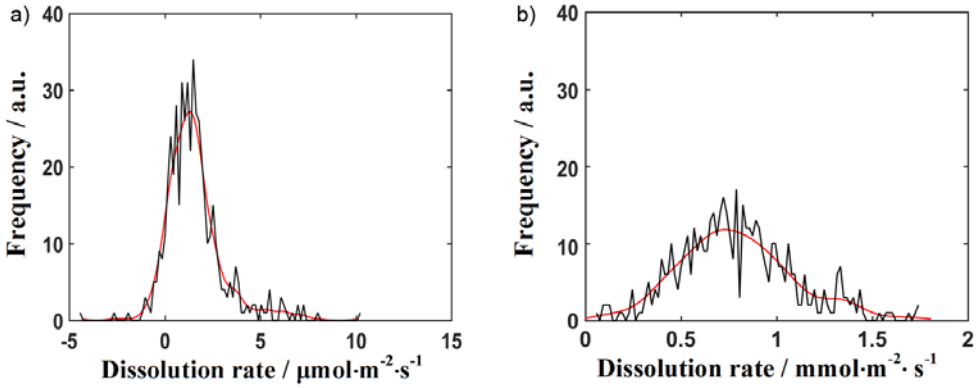

Figure 9: Dissolution rate spectra of region ROI in Figure 3 (a) is the overall dissolution rate spectrum, while (b) is the rate spectrum in the first quarter of a second

4.2 Probable initial dissolution behaviour (a timescale of a few seconds)

As mentioned above, precipitation happens even within the first second of contact with water. Therefore, any dissolution measurement longer than one second is actually a result of the combination of both dissolution and precipitation. By analyzing the data in Figure 8, it can be seen that the average pure dissolution rate of C_3A (in the first quarter of a second) is about 15 to 20 times larger than the rates obtained after two second. So according to Eq. (1) in Section 2.2, the surface height change, $\frac{\Delta h}{\Delta t}$, is about 73.6 ~97.6 nm·s^{-1}. Given the uncertainty of the measurement results shown in Figure 4, the surface height change can reach a maximum value at about 140 nm s^{-1}. If we assume that the pure dissolution rate of C_3A and the pure precipitation rate of hydration product remain constant during the first few seconds, so combined Figure 8 and the value calculated above, the absolute value of precipitation rate should be just slight lower than that of dissolution rate. Within 2 seconds of contact with water, the product layer thickness is estimated to be able to reach 200 ~300 nm. This is close to the value measured under SEM (Figure 7), which is actually slightly higher. This small difference can be attributed to the higher reactivity of the edge region of the sample measured under SEM than the flat regions measured by DHM[19].

5. CONCLUSIONS

- In-situ nanoscale measurement on C_3A dissolution was the first time performed by DHM in flowing deionized water.
- At a flow rate of 34 ml·min^{-1}, C_3A can dissolve at a rate of 500 ~ 1500 mmol·m^{-2}·s^{-1} within the first a quarter of a second after contact with water. After then, crumple foil like hydration product starts to form, which dramatically reduces the dissolution rate of C_3A.

ACKNOWLEDGEMENTS

The authors gratefully acknowledge financial support from National Nature Science Foundation of China via Grant No. U170620242 and 51708108. The authors thank Dr. Jeffrey W. Bullard (Texas A&M University, US) for insightful comments during the preparation of the manuscript.

REFERENCES

[1] Lüttge A. Crystal dissolution kinetics and Gibbs free energy. Journal of Electron Spectroscopy and Related Phenomena, 2006, 150(2-3): 248-259.

[2] Juilland P, Gallucci E, Flatt R, et al. Dissolution theory applied to the induction period in alite hydration. Cement and Concrete Research, 2010, 40(6): 831-844.

[3] Juilland P, Gallucci E. Morpho-topological investigation of the mechanisms and kinetic regimes of alite dissolution. Cement and Concrete Research, 2015, 76: 180-191.

[4] Nicoleau L, Nonat A, Perrey D. The di-and tricalcium silicate dissolutions. Cement and Concrete Research, 2013, 47: 14-30.

[5] Nicoleau L, Nonat A. A new view on the kinetics of tricalcium silicate hydration. Cement and Concrete Research, 2016, 86: 1-11.

[6] Taylor H F W. Cement chemistry. Thomas Telford: London, 1997.

[7] Brand A S, Bullard J W. Dissolution kinetics of cubic tricalcium aluminate measured by digital holographic microscopy. Langmuir, 2017, 33(38): 9645-9656.

[8] Sand K K, Stipp S L S, Hassenkam T, et al. Ethanol adsorption on the $\{10\bar{1}4\}$ calcite surface: preliminary observations with atomic force microscopy. Mineralogical Magazine, 2008, 72(1): 353-357.

[9] Sand K K, Yang M, Makovicky E, et al. Binding of ethanol on calcite: The role of the OH bond and its relevance to biomineralization. Langmuir, 2010, 26(19): 15239-15247.

[10] Feng P, Brand A S, Chen L, et al. In situ nanoscale observations of gypsum dissolution by digital holographic microscopy. Chemical geology, 2017, 460: 25-36.

[11] Brand A S, Feng P, Bullard J W. Calcite dissolution rate spectra measured by in situ digital holographic microscopy. Geochimica et cosmochimica acta, 2017, 213: 317-329.

[12] Alonso M M, Puertas F. Adsorption of PCE and PNS superplasticisers on cubic and orthorhombic C_3A. Effect of sulfate. Construction and Building Materials, 2015, 78: 324-332.

[13] Meredith P, Donald A M, Meller N, et al. Tricalcium aluminate hydration: Microstructural observations by in-situ electron microscopy. Journal of Materials Science, 2004, 39(3): 997-1005.

[14] Ouzia A, Scrivener K. The needle model: A new model for the main hydration peak of alite. Cement and Concrete Research, 2019, 115: 339-360.

[15] Jansen D, Goetz-Neunhoeffer F, Lothenbach B, et al. The early hydration of Ordinary Portland Cement (OPC): An approach comparing measured heat flow with calculated heat flow from QXRD. Cement and Concrete Research, 2012, 42(1): 134-138.

[16] Jennings H M, Pratt P L. An experimental argument for the existence of a protective membrane surrounding Portland cement during the induction period. Cement and Concrete Research, 1979, 9(4): 501-506.

[17] Birchall J D, Howard A J, Bailey J E. On the hydration of Portland cement. Proceedings of the Royal Society of London. A. Mathematical and Physical Sciences, 1978, 360(1702): 445-453.

[18] Fischer C, Luttge A. Beyond the conventional understanding of water–rock reactivity. Earth and Planetary Science Letters, 2017, 457: 100-105.

[19] Arvidson R S, Ertan I E, Amonette J E, et al. Variation in calcite dissolution rates: A fundamental problem?. Geochimica et cosmochimica acta, 2003, 67(9): 1623-1634.